TISSUE ENGINEERING: Part A
Volume 14, Number 1, 2008

DOI: 10.1089/ten.a.2007.0148

Functional Tissue-Engineered Valves from Cell-Remodeled Fibrin with Commissural Alignment of Cell-Produced Collagen

PAUL S. ROBINSON, M.S.,[1] SANDRA L. JOHNSON, B.S.,[1] MICHAEL C. EVANS, Ph.D.,[1] VICTOR H. BAROCAS, Ph.D.,[1] and ROBERT T. TRANQUILLO, Ph.D.[1,2]

ABSTRACT

Heart valve replacements composed of living tissue that can adapt, repair, and grow with a patient would provide a more clinically beneficial option than current inert replacements. Bioartificial valves were produced by entrapping human dermal fibroblasts within a fibrin gel. Using a mold design that presents appropriate mechanical constraints to the cell-induced fibrin gel compaction, gross fiber alignment (commissure-to-commissure alignment in the leaflets and circumferential alignment in the root) and the basic geometry of a native aortic valve were obtained. After static incubation on the mold in complete medium supplemented with transforming growth factor beta 1, insulin, and ascorbate, collagen fibers produced by the entrapped cells were found to coalign with the fibrin based on histological analyses. The resultant tensile mechanical properties were anisotropic. Ultimate tensile strength and tensile modulus of the leaflets in the commissural direction were 0.53 and 2.34 MPa, respectively. The constructs were capable of withstanding backpressure commensurate with porcine aortic valves in regurgitation tests (330 mmHg) and opened and closed under physiological pressure swings of 10 and 20 mmHg, respectively. These data support proof of principle of using cell-remodeled fibrin gel to produce tissue-engineered valve replacements.

INTRODUCTION

THERE IS AN ONGOING quest for a tissue-engineered heart valve, which is especially needed for growing pediatric patients, in whom the common alternatives of inert mechanical valves and bioprosthetic valves are unsatisfactory. The state of the field has been recently reviewed.[1,2] Our approach is based on entrapping cells within a gel of self-assembled native protein fibrils cast in a mold of appropriate geometry.[3,4] Cellularity is achieved directly because cells are entrapped in the gel as it forms, so the approach does not rely on invasion of surface-seeded cells. This approach also has the advantage of using a scaffold composed of native protein fibrils with which cells naturally interact. Traction forces exerted by cells on the relatively compliant network of protein fibrils lead to an extensive cell-induced syneresis of the gel.

We have shown that, when a cell-seeded type I collagen gel is formed within a tubular mold, with channels cut into the central mandrel to form leaflets contiguous with a root segment, then a valvular construct possessing native valve fiber alignment patterns results from the cell-induced gel compaction when all the mold surfaces are nonadhesive.[4] Commissure-to-commissure alignment in the leaflets and circumferential alignment in the root resulted, as demonstrated by anisotropic tensile mechanical properties and histological examination. However, although histology of the leaflets indicated aligned collagen fibrils, it also indicated a lack of other extracellular matrix (ECM) components present in the native valve. The apparent lack of ECM

Departments of [1]Biomedical Engineering and [2]Chemical Engineering and Materials Science, University of Minnesota, Minneapolis, Minnesota.

production by the fibroblasts after contracting and aligning the reconstituted collagen fibrils was consistent with an ultimate tensile strength (UTS) and modulus far below native leaflet values.[5] Although these measures indicated inferior mechanical properties of collagen-based valve equivalents (VEs), the ability to produce valvular constructs possessing alignment properties of native valves makes the tissue-equivalent fabrication attractive, given that fiber alignment is important in specifying anisotropic mechanical properties that confer appropriate function, including the bending[6] and biaxial mechanical properties of heart valve leaflets.[7,8]

In this work, we have thus sought to preserve the VE fabrication approach but to remedy the inferior modulus and strength found when using type I collagen as the biopolymeric scaffold. Previous work in our lab has shown that tissue cells entrapped in a fibrin gel and incubated in medium supplemented with transforming growth factor beta (TGF-β) and insulin exhibit better ECM production than cells entrapped in a collagen gel. The resulting tissue equivalents possess a more tissue-like quality because of enhanced synthesis of collagen,[9] which adopts the alignment of the degrading fibrin,[10] as well as elastic fiber synthesis.[11] The tensile mechanical properties of fibrin-based tissue equivalents approached those of aortic tissue when rat smooth muscle cells were used.[10] Thus, we expected fibrin-based VEs to possess greater modulus and strength than the collagen-based VEs reported in our previous study while retaining the desired commissural alignment in the leaflets and circumferential alignment in the root. In this article, we report on the methods of fabrication and the geometrical, compositional, fiber alignment, uniaxial tensile, and regurgitation properties of fibrin-based VEs.

MATERIALS AND METHODS

Cell culture

Neonatal human dermal fibroblasts (hDFs, Cambrex, Allendale, NJ) were maintained in T-175 culture flasks (Sarstedt, Newton, NC) with Dulbecco's modified Eagle medium (DMEM)/F12 culture medium (Invitrogen, Grand Island, NY) supplemented with 10% fetal bovine serum (FBS, Hyclone, Logan, UT), 100 U/mL penicillin, 100 μg/mL streptomycin, and 2.5 μg/mL amphotericin-β. Cells were incubated at 37°C in 100% humidity and 5% carbon dioxide (CO_2). Cells were passaged at confluency, split, plated at 8600 cells/cm^2, and harvested for use at passage 9.

VE mold

The VE mold is a self-supporting polytetrafluoroethylene structure consisting of an outer housing, a plug, and upper and lower inner mandrels (Fig. 1). Two or 3 open channels that form the leaflets of the bi-leaflet or tri-leaflet VE separate the upper and lower mandrels. The upper mandrel contains an access hole down its axis that allows culture medium into the leaflet channels. This hole is filled with a plug during injection of the gel-forming cell suspension.

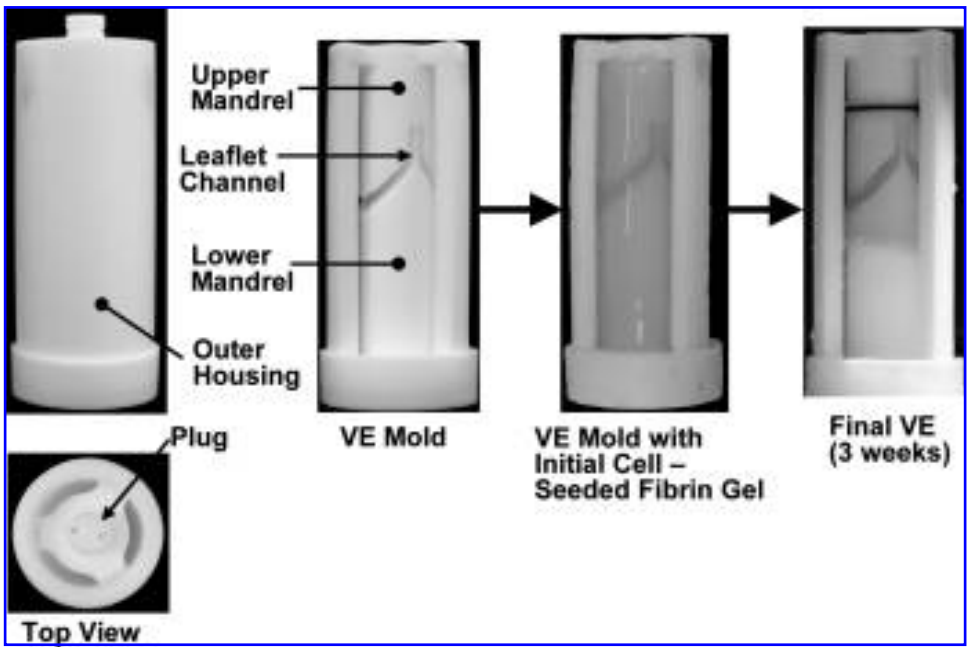

FIG. 1. Valve-equivalent (VE) mold and fabrication. Cell-seeded fibrin-forming solution is injected into the complete mold (left). After gelation, the outer housing and plug are removed and mold and gel placed in culture medium. Culture for 3 weeks with gentle rocking results in a compacted bi-leaflet VE tissue (right).

The diameter of the mandrels and angles of the leaflet channels are consistent with the VE mold previously described by Neidert *et al.*,[4] which was designed to mimic the dimensions of the human aortic valve.

Initial (small strain) gel compaction in this mold was simulated by using the mold geometry in a 3-dimensional (3D) finite element implementation of the anisotropic biphasic theory (ABT) model of Barocas and Tranquillo.[12] The 3D simulation code was recently validated in predicting fiber alignment patterns during initial compaction in other geometries.[13] In the VE application, a boundary condition associated with the leaflet channel lies on a noncoordinate surface, requiring a modification to the code to enforce a free-slip condition of the gel along the channel surface. The full set of boundary conditions along with the modification to the code in Oshumi *et al.*[13] is included in the Appendix. The simulation results are qualitatively compared with the alignment patterns measured in the VEs to assess the code's use as a tool for future VE design.

Fibrin gel preparation

Cell-seeded fibrin gel was formulated by mixing hDFs suspended in DMEM into a solution of bovine fibrinogen (Sigma) in 20 mM 4-(2-hydroxyethyl)-1-piperazineethanesulfonic acid-buffered saline. A mixture of bovine thrombin (Sigma) and calcium chloride in DMEM was then added to the fibrinogen–cell mixture. All components were at room temperature. Final concentrations of this suspension were 6.6 mg/mL fibrinogen, 1.1 U/mL thrombin, 5.0 mM Ca^{++}, and 500,000 cells/mL. Suspensions were mixed well by pipette action and injected into the VE molds within 1 min while still liquid.

VE fabrication

For VE fabrication, mold parts were sterilized using 70% ethanol and then coated with Pluronic F-127 (Sigma). Dacron rings (St. Jude Medical, St. Paul, MN) were placed around the lower and upper extremes of the mandrels. Molds were assembled and sealed with sterile vacuum grease (Dow Corning, Midland, MI). After injection of the suspension, the top of the mold was sealed with a rubber plug and the molds placed horizontally on a roller in an incubator at 37°C, 5%CO_2, and 100% humidity. Molds were rotated at 0.4 rpm for a gelation period of 30 min to mitigate settling of cells and gel. After gelation, the outer housing and plugs were removed, and constructs were placed horizontally in culture medium comprised of high-glucose DMEM supplemented with 10% FBS (Hyclone), 100 U/mL penicillin, 100 μg/mL streptomycin, 2.5 μg/mL amphotericin-β, 1 ng/mL TGF-β, 2 μg/mL insulin, and 50 μg/mL ascorbic acid. VEs were cultured with gentle rocking to ensure even distribution of medium outside the construct and within the leaflet channel via the access hole. A 70% medium change was performed 3 times per week.

Constructs were cultured for 21 to 25 days (3-week bi-leaflet VEs, $n = 7$ and 3-week tri-leaflet VEs, $n = 3$) or 35 days (5-week bi-leaflet VEs, $n = 6$), after which they were harvested and assayed as described below. At 14 days of incubation, #3 silk suture (Deknatel, Research Triangle Park, NC) was tied around the upper Dacron ring to clamp the upper portion of the VE construct onto the mold, preventing axial shortening of the upper root segment below the top of the leaflet channels. Failure to do so resulted in insufficient root tissue for VE testing and loss of leaflet coaption. Figure 1 depicts the fabrication process with initial and final construct appearance.

Pressurization

VEs were tied onto threaded hose barbs using #3 silk suture around the upper Dacron ring and placed in a bath of phosphate buffered saline (PBS). The VE was attached in series to a pressure transducer (Harvard Apparatus, Holliston, MA) and a 60-cc syringe using silicon tubing. The lower portion of the VE was free in the bath. The syringe and tubing were filled with Hank's balanced salt solution (HBSS) containing phenol red, which enabled visualization of any leaks in the VE or its tube attachment. After determining that no leaks were present, the syringe plunger was cyclically moved back and forth to pulse the VE at varying rates and just enough pressure to open and close the VE. After pulsation, the syringe plunger was depressed rapidly to pressurize the VE at approximately 100 mmHg/s until the VE failed by no longer sustaining pressure. Maximum backpressure was defined as the maximum pressure recorded by the transducer during this test.

VE dissection

After pressurization, VE's were transected longitudinally at one of the commissures and the leaflets resected. Fiber alignment in the root and leaflets was measured using polarized light imaging, as described by Tower *et al.*[14] Tissue was then dissected as follows. Approximately one third of 1 leaflet was cut off and used for histologic analysis. From this same leaflet, strips were cut from the free edge along the circumferential direction and from the belly along the radial direction. A strip was also cut from the belly of the other leaflet along the circumferential direction. Preliminary studies showed no significant differences between the 2 leaflets in a VE. Strips were also cut from the upper root (from the area behind the leaflets) along the circumferential and axial directions. Three-mm (leaflets) or 7-mm (roots) punch biopsies were taken from the free edge and belly areas of the leaflets and upper root for compositional analysis. A rectangular area encompassing portions of the upper and lower root and leaflet attachment site was cut from each root for histologic analysis.

Histology

Histology samples were fixed in 4% paraformaldehyde, infiltrated with sucrose, frozen in optimal cutting temperature compound (Tissue-Tek, Torrance, CA) and sectioned.

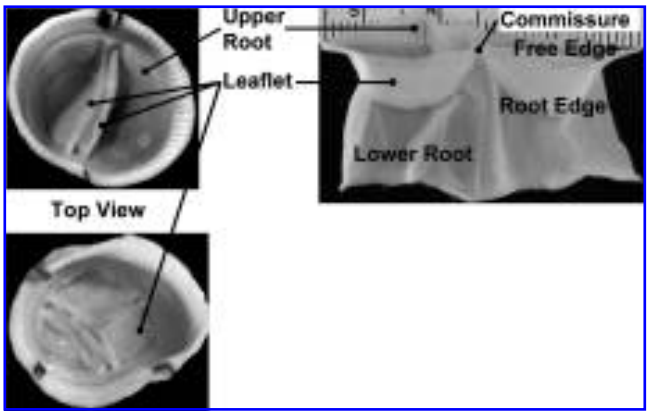

FIG. 2. Fibrin-based valve equivalents (VEs). After 3 and 5 weeks of culture, bi-leaflet VEs were created that had 2 coapting, cusp-like leaflets attached to a cylindrical root. Left, top (aortic) side view. Right, VE cut axially through one commissure and opened flat for luminal view. Lower left, top view of tri-leaflet VE.

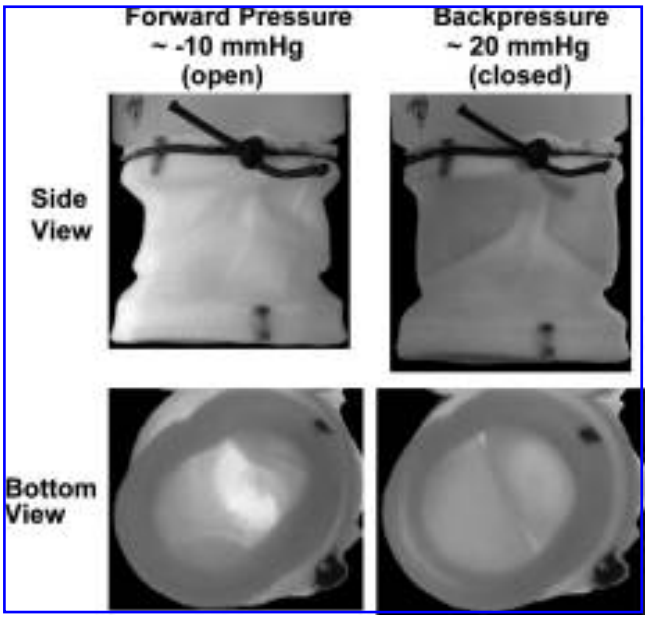

FIG. 3. Valve-equivalent (VE) pressurization. Side view of a typical 3-week VE. Left, VE open and allowing fluid flow. Right, VE closed with slight pressurization.

In a subset of VEs ($n = 3$ each time point), non-collagen protein was removed beforeembedding and freezing by digestion in 0.25% trypsin in 0.1% ethylenediaminetetraacetic acid in HBSS overnight at room temperature. Fiber alignment images of the samples were taken before and after trypsin digestion using polarized light imaging.[14] In other VEs, trypsin digestion was performed after sectioning, with adjacent sections serving as undigested controls. All sections were stained with Lillie's trichrome.[15]

Composition

Collagen content was quantified using the hydroxyproline assay of Stegeman and Stadler.[16] Elastin content was measured using the modified ninhydrin assay.[11,17] Collagen per sample was calculated using a conversion factor of 7.46 μg of collagen per μg of 4-hydroxyproline.[18] Collagen and elastin content were measured in the strips used for mechanical testing and in circular biopsies taken from the leaflets and roots. Sample volume was calculated using the length and width of the strips or the diameter of the biopsies and the measured thickness of each sample (see uniaxial testing, below). Collagen and elastin contents were calculated as the amount per unit volume in each sample.

Deoxyribonucleic acid (DNA) content in the circular biopsies was quantified using a modified Hoechst assay.[19] Cell numbers were obtained from DNA content assuming 7.6 pg of DNA per cell.[20] Cellularity was calculated as the number of cells per unit volume.

Uniaxial tensile testing

Stain lines to demarcate a gauge region of approximately 4 mm were placed on each tissue strip using 6–0 silk suture dipped in Verhoeff's stain. The thickness of each strip was calculated as the average of 3 measurements along the gauge region taken with a low-force probe. Strips were placed in compressive grips, attached to actuator arms and load cells of a materials testing system (Instron, Cambridge, MA), and straightened to a load of 0.005 N. This position was used as the reference length of the strip. After 10 cycles of 0 to 10% strain at 0.3%/s, samples were allowed to equilibrate for 60 s and then subjected to a stress relaxation test at 10% strain for 300 s. After relaxation, a quasi-static ramp to failure test was performed at a rate of 0.3%/s. High-resolution digital images were captured of the reference position and ramp-to-failure test. The reference image was used to measure initial specimen width and gauge length, defined as the distance between the centroids of the stain lines. Local average sample stretch was determined by measuring the displacements of the centroids of the stain lines in each image during the ramp test. All image measurement and calculations of strain, stress, tension, Young's modulus, and membrane stiffness, based on initial specimen dimensions, were performed using custom applications in Matlab software (Mathworks, Natick, MA). Tension and membrane stiffness were reported in addition to stress and modulus as relevant measures of mechanical function in complex composite tissues[8,21] and to allow comparison of our data with that from previous studies.

Native valve tissue

Porcine hearts ($n = 8$) were obtained fresh-frozen from the Minnesota Department of Agriculture. The aortic valves were resected and subjected to the same pressurization, mechanical, and compositional analyses as VE tissue. Strips for mechanical testing and 3-mm punch biopsies were cut

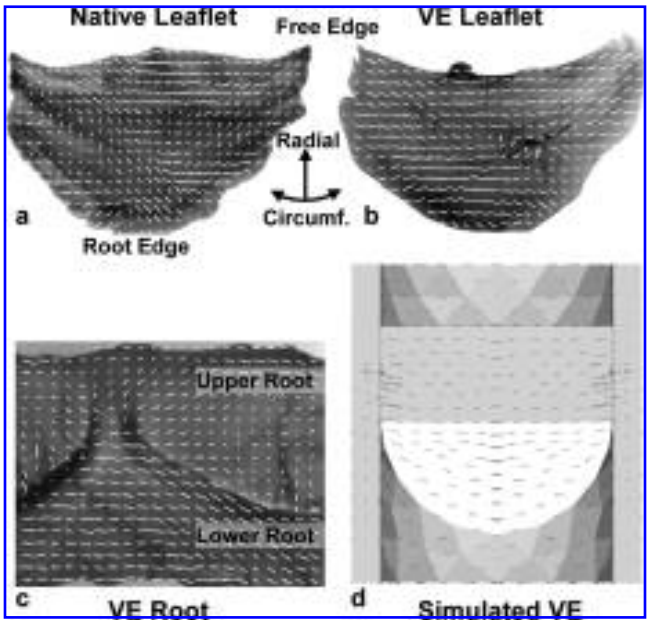

FIG. 4. Valve-equivalent (VE) fiber alignment. Fiber alignments of (**A**) native leaflet, (**B**) 3-week VE leaflet, and (**C**) 3-week VE root as determined using polarized light imaging. The orientations of the white lines correspond to the local average fiber direction, and their lengths are proportional to the local average retardation, a measure of the fiber alignment strength. (**D**) anisotropic biphasic theory (ABT) simulation of gel compaction in the mold. Black lines indicate principal fiber alignment directions in the root (triangulated gray areas) and leaflet (solid white and gray interior areas). The ABT is limited to small strain (<15%), so the gel has compacted downward only slightly through the leaflet channel. (Simulated gel indicated as the solid gray area is actually compacted or degraded by 3 weeks of incubation.)

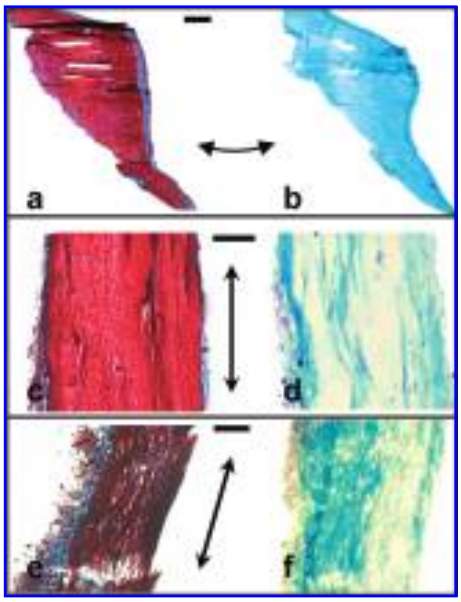

FIG. 5. Valve-equivalent (VE) histology. (**A**) 10-μm planar section of 5-week VE leaflet, (**C**) 25-μm cross-section of 5-week VE leaflet belly region, (**E**) 50-μm cross-section of 3-week VE lower root. (**B, D, E**) Sections adjacent to **A, C, E** after digestion in trypsin. All sections stained with Lillie's trichrome: green = collagen, black = elastin, blue/black = cell nuclei, red = other extracellular matrix (fibrin). Double arrow indicates circumferential direction. Bar = 1 mm (**A, B**), 50 μm (**C, D**), or 100 μm (**E, F**).

from the noncoronary leaflet and the noncoronary sinus area of the root.

Statistics

Circumferential and radial–axial mechanical properties in the leaflets and roots were compared using a paired Student *t*-test. Mechanical and compositional differences between 3-week VEs, 5-week VEs, and native aortic valve tissues were examined with one-way analysis of variance followed by Fisher's least significant difference *post hoc* test. Significance was set at $p < 0.05$.

RESULTS

We successfully created functional VEs using the mold shown in Figure 1 and the tissue-equivalent fabrication process described above. Typical bi-leaflet VEs are shown in Figures 2 and 3. They consisted of a cylindrical root section transected by 2 coapting leaflets. The leaflets were cusp-like (Fig. 2), exhibiting a shape similar to that of native aortic valve leaflets. Tri-leaflet VEs had a similar appearance, except with 3 coapting leaflets (Fig. 2C). After 3 weeks of culture, VEs were robust enough to be handled, pressurized, and tested as described above. After 5 weeks of culture, VE tissue was grossly similar except that, in most VEs, a defect formed in the root just above the leaflet attachment. This defect was due to excessive contraction of the tissue against the edge of the upper mandrel of the mold. This area of thin tissue led to failure of the root at low pressures at these specific points. Therefore, no back-pressure data were collected for the 5-week VEs, although all other assays were performed. Larger leaflets in the bi-leaflet VEs produced more localized tissue allowing all the described assays to be performed on single leaflets. Therefore, bi-leaflet VEs were used in generating the majority of the results, and all results reported here refer to bi-leaflet VEs unless explicitly stated otherwise.

Pressurization

VEs were observed to open and close repeatedly with the application of fluid pressure gradients. VEs appeared closed at a nominal pressure of 20 mmHg, with a slight expansion of the upper root also observed at this pressure (Fig. 3), where positive pressure is defined as pressure against the valve (back-pressure). VEs appeared fully open at a nominal pressure of –10 mmHg. VEs could be pulsed at frequencies

ranging from 0.5 to 2 Hz with no observable loss of leaflet coaptation.

VEs incubated for 3 weeks sustained a maximum backpressure similar to that of porcine aortic valves. When rapidly pressurized until failure, 3-week VEs and porcine aortic valves failed at pressures of 334 ± 84 and 324 ± 104 mmHg (mean $\pm$ standard deviation, $p = 0.5$), respectively. VEs failed either by dilation of the VE root to a point where leaflet coaptation could no longer be maintained ($n = 3$) or by tearing of the VE tissue in the root ($n = 4$). All porcine aortic valves failed by dilation of the root to a point where the leaflets could no longer coapt.

Fiber alignment

VE leaflets exhibited a fiber alignment pattern similar to that of native leaflets. This is shown in Figure 4, where fiber alignment maps of 2 typical leaflets overlay their brightfield view. The orientation of the white lines on the images correspond to the local area average fiber direction, and their lengths are proportional to the local average retardation, a measure of fiber alignment strength. In VE and native tissue, the predominant alignment direction is circumferential (commissure to commissure). Alignment patterns were similar in 3-week and 5-week leaflets (as well as in 3-week tri-leaflet VEs—not shown). The alignment patterns measured in the VE tissue correspond qualitatively with the ABT model simulations (Fig. 4D).

Circumferential alignment was observed in VE roots (Fig. 4C). Alignment was stronger in the lower root, the area below the leaflets, than in the upper root, the area behind the leaflets that corresponds to the sinus area of the native valve. Similar alignment patterns were observed in 3-week and 5-week bi-leaflet VEs and 3-week tri-leaflet VEs. Alignment maps were not generated for native root because of a limitation of the polarimetry system requiring more light transmission than could be achieved.

Histology

Cells and cell-produced collagen were observed to be located throughout the VE leaflet and root tissue. Figure 5A shows a 10-μm planar section of a VE leaflet stained with Lillie's trichrome. When an adjacent section was trypsin-treated to remove all but the collagen and elastin ECM components (Fig. 5B), collagen was observed to be distributed throughout the entire tissue. Cross-sections of leaflets and root (Fig. 5C, E) showed cells distributed through the tissue, with more cellular regions at the surfaces. Many of these cells were elongated along the circumferential direction, as seen in the thin sections (Fig. 5C, D). In adjacent cross-sections, trypsin digestion revealed that collagen was distributed throughout the entire thickness of the tissue (Fig. 5D, F).

This collagen was coaligned with the cell-aligned fibrin. Alignment maps generated before and after trypsin digestion on whole tissue pieces yielded similar fiber alignment patterns (Fig. 6). This was observed in 3-week and 5-week VEs. Twenty-five-μm cross-sections of leaflet and lower root tissue (Fig. 5) corroborate the alignment map data, showing fibers aligned circumferentially. Trypsin digestion on adjacent sections revealed collagen fibers also aligned circumferentially (Fig. 5).

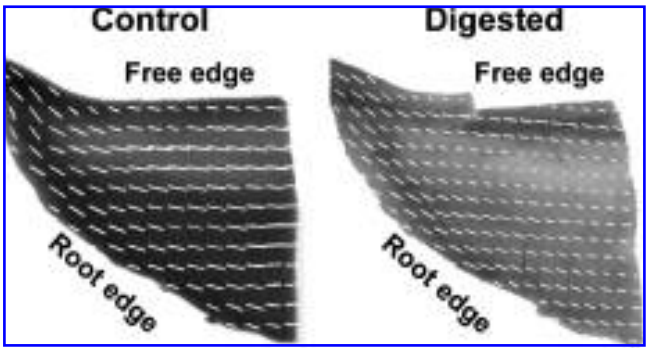

FIG. 6. Valve-equivalent (VE) collagen alignment. Fiber alignments of a portion of a 5-week VE leaflet (**A**) before and (**B**) after digestion in trypsin to remove the noncollagenous proteins. Similar alignment patterns show that the cell-produced collagen adopts the same alignment as the fibrin.

Composition

Cell-produced collagen was measured in VE tissue at 3 and 5 weeks (Fig. 7). Collagen concentration increased in the leaflet free edge between 3 and 5 weeks ($p = 0.02$). There was no increase in collagen concentration in the leaflet belly or VE root between 3-week and 5-week VEs. VE leaflet and root tissue had a much lower collagen concentration than the porcine aortic valve tissue ($p < 0.001$, Figure 7). Negligible elastin production was measured.

hDFs proliferated during VE culture. Cellularity in the leaflet-free edge was similar for 3-week and 5-week VEs, but cellularity in the leaflet belly increased between 3 and 5 weeks ($p = 0.002$, Fig. 7). Root cellularity was similar at both time points. Ranging from 78×10^6 to 148×10^6 cells/mL, these numbers were much higher than the effective initial cellularity of 5×10^6 cells/mL, given that the initial cell density was 0.5×10^6 cells/mL and the final VE tissue volume was approximately one-tenth the initial gel volume. Thus, approximately 5 cell population doublings occurred. VE cellularity was approximately half of native cellularity in the leaflet belly ($p < 0.005$) and equal to native cellularity in the root.

Uniaxial mechanical testing

Figure 8 and Tables 1 and 2 summarize the uniaxial mechanical properties measured for VE and pig aortic tissue. In general, the mechanical properties of 3-week and 5-

Table 1. Valve Equivalent (VE) Leaflet Mechanical Properties and Composition

	3 week VE	*5 week VE*	*Native Valve*
Thickness, mm			
Free	0.23 ± 0.04	0.29 ± 0.09	0.32 ± 0.09
Belly	0.34 ± 0.04	0.34 ± 0.10	0.45 ± 0.06
UTS, kPa			
Circumferential, free	584 ± 191	530 ± 178	1148 ± 262*
Circumferential, belly	523 ± 80	634 ± 376	1101 ± 200*,§
Radial, belly	426 ± 247	215 ± 128	632 ± 208†
Modulus, kPa			
Circumferential, free	1447 ± 337	2343 ± 662‡	11084 ± 1843*
Circumferential, belly	1121 ± 369§	1846 ± 1107§	14885 ± 5155*,§
Radial, belly	581 ± 392	386 ± 204	2477 ± 886*
Maximum Tension, N/m			
Circumferential, free	139 ± 59	150 ± 70	357 ± 107*
Circumferential, belly	179 ± 34§	155 ± 27§	407 ± 140*
Radial, belly	96 ± 31	63 ± 26	276 ± 63*
Membrane Stiffness, N/m			
Circumferential, free	338 ± 131	684 ± 262‡	3486 ± 1112*
Circumferential, belly	385 ± 171§	591 ± 185§	6531 ± 1631*,§
Radial, belly	143 ± 43	115 ± 49	1090 ± 277*
Collagen content, mg/ml			
Free	5 ± 3	12 ± 5‡	95 ± 29*
Belly	5 ± 2	10 ± 5	84 ± 18*
Cellularity, 10^6cells/ml			
Free	115 ± 39	101 ± 36	n/m
Belly	78 ± 24	115 ± 41‡	215 ± 48*

* = native > 3 week and 5 week VE, $p < 0.01$
† = native > 5 week VE, $p = 0.002$
‡ = 5 week > 3 week VE, $p < 0.02$
§ = circumferential > radial, $p < 0.015$
n/m = not measured

week VEs were similar, with the only differences measured between them being in the modulus and membrane stiffness of the free edge of the leaflet in the circumferential direction (5 week $>$ 3 week, $p = 0.01$) and in the maximum tension of the root in the axial direction (3 week $>$ 5 week, $p = 0.01$). The tensile properties of 3-week trileaflet VE leaflet bellies in the circumferential direction (UTS $= 487 \pm 90$ kPa, modulus $= 1754 \pm 890$ kPa) and radial direction (UTS $= 266 \pm 1$ kPa, modulus $= 529 \pm 60$ kPa) were similar to 3-week bi-leaflet VE properties. Root properties also showed no difference between trileaflet and bi-leaflet VEs.

Porcine aortic tissue had higher values for all properties shown except leaflet UTS in the radial direction and root modulus in the circumferential and axial directions. VE leaflet UTS and maximum tension in the circumferential direction were about half of native values, on average. In the radial direction, VE leaflet maximum tension was approximately one-third that of native tissue. VE leaflet moduli and membrane stiffnesses in all directions ranged from one-tenth to one-fifth of native values. Root moduli in both directions were similar for VE and native tissue. Membrane stiffnesses, however, were 10 to 20 times higher in native tissue because of native root being much thicker than VE root. Failure properties (UTS, maximum tension) were not obtained for native root, because many root specimens exceeded the extension limit of the testing protocol (15 mm) or the load limit of the force transducer (5 N).

Corresponding to the fiber alignment shown in Figures 5 and 6, VE tissue exhibited a mechanical anisotropy similar to that of native tissue. In the leaflets, modulus and membrane stiffness were higher in the circumferential direction than in the radial direction for VE and native tissue. Furthermore, the index of anisotropy, defined as the ratio of the circumferential to radial property value, was similar for modulus (3.1 ± 1.9, 3 week; 3.3 ± 1.8, 5 week; 4.7 ± 1.0, native; $p = 0.2$) and membrane stiffness (3.0 ± 1.7, 3 week; 4.9 ± 1.9, 5 week; 3.3 ± 1.3, native; $p = 0.2$). The lack of significant anisotropy in the root mechanical properties of all groups also indicted VE and native valve similarity.

Table 2. Valve Equivalent (VE) Root Mechanical Properties and Composition

	3 week VE	*5 week VE*	*Native Valve*
Thickness, mm	0.31 ± 0.08	0.20 ± 0.08	2.81 ± 0.38
UTS, kPa			
Circumferential	154 ± 46	173 ± 90	n/m
Axial	185 ± 40	163 ± 86	n/m
Modulus, kPa			
Circumferential	858 ± 261	861 ± 423	1255 ± 562
Axial	869 ± 420	806 ± 421	1027 ± 407
Maximum Tension, N/m			
Circumferential	47 ± 14	33 ± 13	n/m
Axial	54 ± 15	$28 \pm 13^{\dagger}$	n/m
Membrane Stiffness, N/m			
Circumferential	260 ± 82	169 ± 62	3021 ± 1365*
Axial	252 ± 130	140 ± 76	2771 ± 783*
Collagen content, mg/ml	10 ± 3	12 ± 6	36 ± 9*
Cellularity, 10^6cells/ml	148 ± 50	121 ± 29	152 ± 50

*= native > 3 week and 5 week VE, $p < 0.01$
† = 3 week > 5 week VE, $p < 0.02$
n/m = not measured

DISCUSSION

The method described here creates functional tissue-engineered VEs from fibrin gel that is structurally and compositionally remodeled using entrapped human dermal fibroblasts. These VEs have a gross structure and dimensions similar to those of a human aortic valve. Furthermore, the VEs exhibit the hallmark commissural fiber alignment and anisotropic mechanical properties in the leaflets and a maximum back-pressure loading comparable with that of native aortic valves. This method represents a significant step forward in creating living-tissue heart valve replacements.

In this study, VE functionality was assessed using pressurization. During repeated cycles of opening and closing, VEs and porcine aortic valves were observed to be fully open and to allow flow at –10 mmHg. This compared well with the reported pressure drops in an open aortic valve during systole of –5 to –10 mmHg.[22,23] When pressurized to failure at a physiologically relevant rate of 100 mmHg/s, VEs sustained the same maximum back pressure ($\sim$330 mmHg) as porcine aortic valves. These data indicate the ability of these VEs to withstand the pressure demands of a normal cardiac cycle.

Underlying fiber alignment is also important in determining the eventual functionality of tissue-engineered valves. Several investigators have shown significant differences in simulated valve function when including anisotropic structure and mechanical properties in valve mathematical models.[24,25] Such differences include reduction of peak stresses,[26,27] increase in leaflet deformation,[27] reduction in leaflet bending moment during systole,[26,27] and improved pressure-radius predictions in arterial wall.[28,29] Therefore, it is important to mimic this structural and mechanical anisotropy in tissue-engineered valve constructs.

As intended with our casting mold design and predicted by the ABT-based simulation, the cell-induced contraction of the fibrin gel resulted in leaflet and root fiber alignments similar to those of native aortic valves. Histological analysis of VE-tissue cross-sections confirmed the fiber alignment patterns measured using polarimetric alignment imaging. Furthermore alignment imaging and histological sections of VE tissue digested to remove noncollagenous proteins revealed that the cell-produced collagen was coaligned with the bulk tissue (residual fibrin and other cell-produced ECM fibers). Our fabrication method thus allows for the *in vitro* growth of tissue with prescribed alignment in the complex geometry of a heart valve. With greater collagen and elastin deposition, this method might yield tissue-engineered valves that closely mimic native-valve mechanical function before implantation, although such function might result upon further remodeling *in vivo* with the valve constructs described here. As indicated, longer incubation time under the current incubation conditions is not a viable means of achieving greater collagen and elastin deposition because of the tissue damage that occurs along the edge of the upper mandrel where the leaflet channel intersects the outer cylindrical surface of the mandrel. This damage appears to result from the sustained traction forces exerted by the cells leading to the tissue being stressed around that edge; localized ECM proteolysis in response to stress concentration may play an exacerbating role. Extended incubation times would require identifying conditions that diminish traction force without inhibiting ECM production.

Cellularity in 3-week and 5-week VEs was comparable with that of native heart valve. The histological sections indicated elongated cells throughout the VE tissue. Living cells are important in heart valves for maintaining valve matrix tissue structural and compositional integrity;[30] living

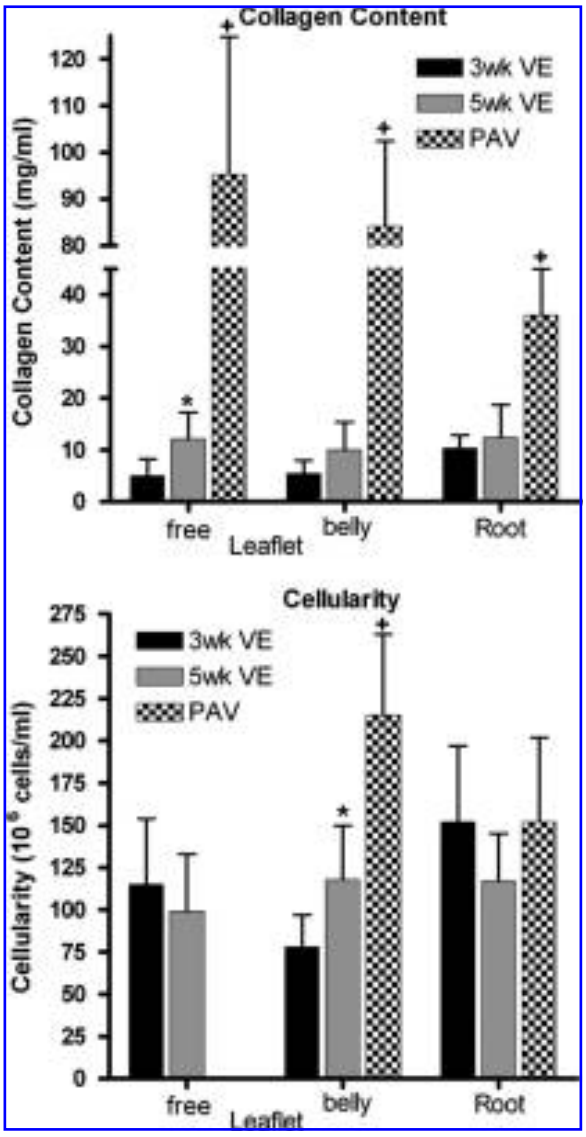

FIG. 7. Valve-equivalent (VE) composition. Collagen content and cellularity of VE tissue at 3 and 5 weeks of static incubation and porcine aortic valve tissue (PAV). +PAV > 3-week and 5-week VEs, $p < 0.01$; *5-week VEs > 3-week VEs, $p < 0.02$.

cells within a VE would allow it to further remodel *in vivo* to strengthen the matrix and potentially grow with a patient. The neonatal hDFs used here imply a nonautologous cell source. Neonatal hDFs are the tissue cells used in the production of the bioartificial skin Apligraf (Organogenesis, Canton, MA). In clinical trials, there was no evidence of clinical rejection of Apligraf, and immunological tests indicated no humoral or cellular response to the fibroblasts.[31] Neonatal cells are generally better ECM-producing cells than their adult counterparts. So although the immunogenicity question would have to be assessed in this cardiovascular application, the Apligraf precedent motivates the use of allogenic neonatal hDFs, because the VE could then be similarly prefabricated and not rely on a patient biopsy for the tissue cell source.

The hDFs used in this study represent a readily available cell source (allogenic or autogenic) for future clinical and animal study applications. Others have investigated this cell source[32,33] but not in fibrin-based constructs, although the related myofibroblast, either dermal- or vascular-derived, has often been used instead of valve interstitial cells (VICs) for heart valve tissue engineering.[34–38] Although VICs are the resident valve population, they are much more difficult, and dangerous in the case of an autogenic source, to procure. In previous studies, we have found a similar degree of collagen production between hDFs and VICs in a model fibrin gel–based construct (adherent discs).[39] Even though hDFs may differ morphologically and functionally from VICs, this study shows that this readily available cell source can be used to create functional valve constructs. It is likely that the hDFs in these constructs have adopted a myofibroblasts phenotype. This has been shown in previous studies using fibrin-based disc constructs under the same culture conditions used in this study. At 3 weeks of culture, cells stained positive for vimentin and smooth-muscle actin.[39]

The present *in vitro* VE characterization did not require the VEs to be endothelialized. We have assessed the adhesion of endothelial cells (ECs) to remodeled fibrin by neonatal SMCs[40] and hDFs (unpublished studies). We found that an EC monolayer can be readily created in 48 h and that 95% of the ECs are retained after 48 h exposure to pulsatile flow at physiological shear stress (15 dyne/cm^2). If it proves necessary to endothelialize the VE to eliminate thrombus formation, there is reason to believe that a stable neoendothelium can be formed with the resulting tissue surface following long-term fibrin remodeling. However, given the antigenicity of ECs, there is no alternative at present to using ECs derived from the patient, either as primary cells or via progenitor cells.

Fibrin-based VEs represent an improvement in VE fabrication from earlier work using cell-seeded collagen gel. In Neidert *et al.*,[4] bi-leaflet collagen-based VEs were fabricated that possessed circumferential fiber alignment and a leaflet UTS and modulus in the circumferential direction of 320 kPa and 28 kPa, respectively, after 3 weeks of incubation. Fibrin-based VEs possessed the same fiber alignment patterns but with better mechanical properties (530 kPa UTS, 2343 kPa modulus).

The strength and stiffness measured in VE leaflets was less than those of native values. VE strength, as measured according to UTS and maximum tension, was approximately 50% of native strength. VE stiffness, as measured according to modulus and membrane stiffness, was approximately 15% of native stiffness, although the UTS and maximum tension of VE leaflets were comparable with the maximum stress (500 kPa) and tension (175 kPa) in the leaflet during normal aortic valve function estimated according to several *in vivo* studies and mathematical simulations.[27,41,42] Although much thinner, VE roots and native valve roots possessed similar

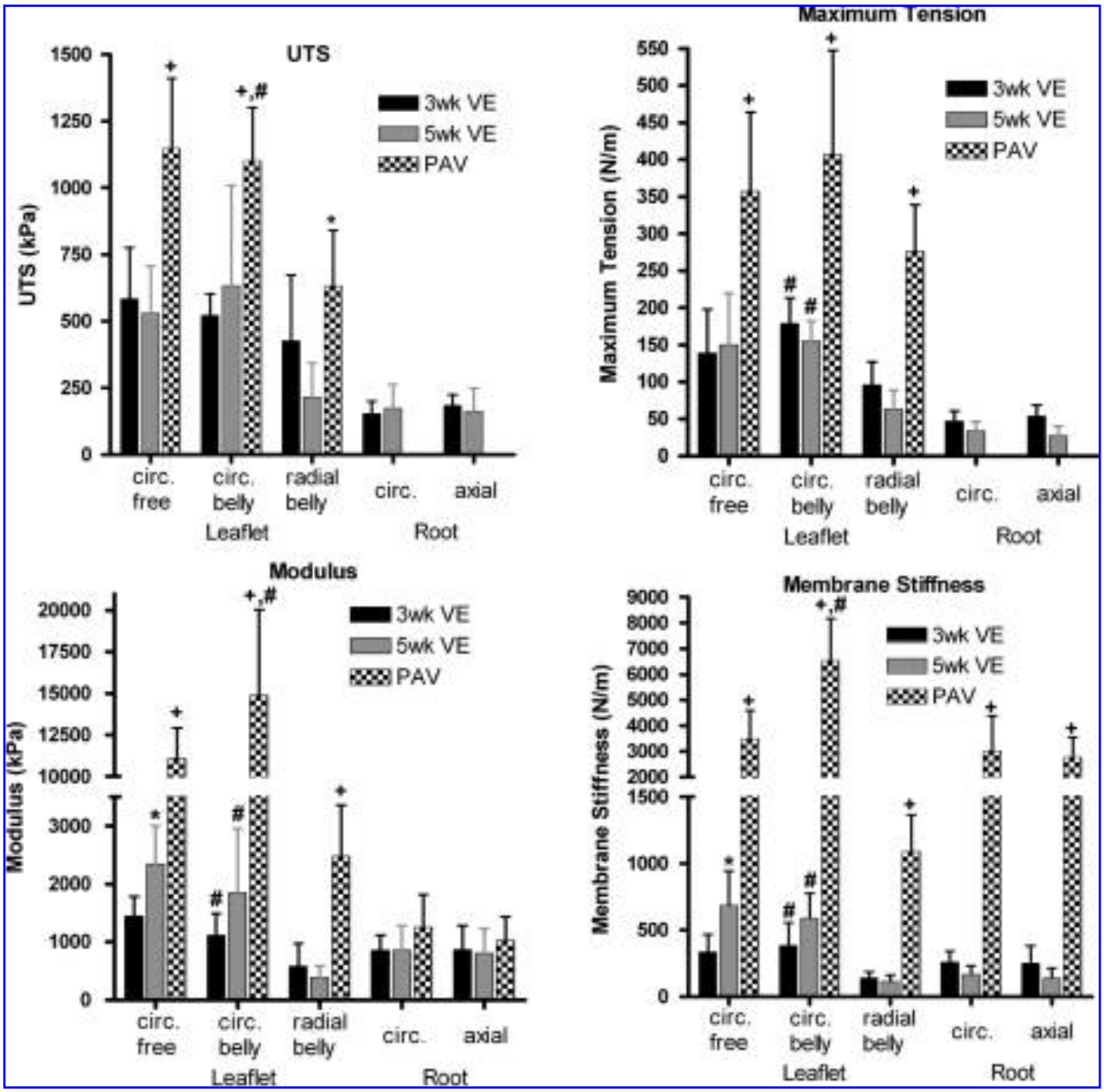

FIG. 8. Valve-equivalent (VE) mechanical properties. Mechanical properties measured by uniaxial tension testing of strips of tissue cut from 3- and 5-week VEs and porcine aortic valves (PAVs). +PAV > 3-week and 5-week VEs, $p < 0.01$; # circumferential property > radial or axial property, $p < 0.02$, *5-week VEs > 3-week VEs, $p < 0.02$.

moduli. This has implications for prospective intraluminal implantation of the VE; given the same stress due to lumen pressurization, the VE root will distend similar to native aortic root because of the similar moduli. Future studies with VE constructs implanted interpositionally may require a design change to create thicker roots. In summary, the mechanical properties observed in 3-week VEs represent tissue that can potentially function within the physiologic demands of aortic heart valves.

The native valve contains a significant number of elastic fibers that are important in the tissue elasticity required to recover from the large deformations that the leaflets undergo during cardiac cycle.[43] However, there was a negligible deposition of elastic fibers in the VEs fabricated in these studies. Nonetheless, there was elasticity inherent in the VE tissue. There was no visible creep observed during the preconditioning phase of the uniaxial mechanical testing in this study. Also, similarly prepared tubular constructs have been subjected to cyclic distension at 1 Hz for up to 3 weeks with no apparent creep (unpublished data). Therefore, these VE tissues may have the requisite elasticity to function adequately. Residual fibrin[44] or other cell-produced ECM could

bestow this. For example, our immunogold-labeling studies of similarly prepared and cultured constructs formed as adherent hemispheres[9] revealed that an extensive network of fibronectin fibrils is formed in this system (unpublished studies), which can strongly modulate tensile mechanical properties.[45]

The results presented here show that, even without potential improvements, this method creates VEs that initially can withstand the pressures, stresses, and deformations required of a functioning aortic heart valve. Although bi-leaflet VEs were mainly investigated here for convenience and comparison to our collagen-based VE construct results,[4] we fabricated tri-leaflet VEs with this process in a similar mold with 3 channels. Their tensile mechanical properties are statistically the same as those of the bi-leaflet VEs, although it is likely that their pressure-flow characteristics are much more favorable. Future studies on bi-leaflet and tri-leaflet VEs will further elucidate functional differences between the 2 geometries. Although still suboptimal compared with native heart valve tissue in terms of tensile mechanical properties and collagen content, the bi-leaflet VEs presented here are comparable with those of other tissue-engineered heart valves created with synthetic polymers and incubated statically for similar time periods,[37,46] including those successfully implanted in a large-animal model.[34,46] Several other studies using synthetic polymers have shown improvements in tissue-engineered heart valve properties when constructs were subject to cyclic stretching during incubation.[37,47] We have made similar observations in other fibrin-based constructs. Therefore, we expect that as dynamic incubation conditions and implant studies progress, VE properties will continue to improve and VEs will perform adequately *in vivo*.

ACKNOWLEDGMENTS

The authors thank Naomi Ferguson (University of Minnesota) for cell-culture support and Drs. Neeser and Tsehaye (Minnesota Department of Agriculture) for providing porcine hearts. Funding provided by National Institutes of Health (BRP HL71538 to RTT).

APPENDIX – IMPLEMENTATION OF THE 3-D ABT MODEL

The governing equations and the details of the 3-D solution scheme are given elsewhere,[13] so only the novel aspects applied to the valve are given here. The previous study implemented a 3-dimensional scheme that could only incorporate boundary conditions on the displacement of 3 types: velocity and displacement (all 3 components of position or displacement specified), free (no shear or normal stress at the surface), and symmetry (no shear stress or normal displacement). Although those 3 conditions encompass a wide range of situations, the interaction between the leaflet and the mold surface is a non-adhesive contact condition, in which

$$\begin{aligned} n_i t_j \sigma_{ij} &= 0 \\ (n_j u_j)(n_i n_j \sigma_{ij}) &= 0 \\ (n_j u_j) + (n_i n_j \sigma_{ij}) &< 0 \end{aligned} \tag{1}$$

where n and t are the normal and tangents to the surface, σ is the stress on the surface, and u is the vector pointing from the wall to the surface. The first condition requires no shear stress. The second condition requires that the surface be in contact with the wall ($n_j u_j = 0$) or that there be no normal stress ($n_i n_j \sigma_{ij} = 0$ because the surface is not in contact and thus free). The third condition requires that the surface be away from the wall ($n_j u_j < 0$) or that the surface be in compression ($n_i n_j \sigma_{ij} < 0$). Rather than enforcing these conditions formally, which is a considerable challenge, we implemented a penalty scheme in which an artificial separation-dependent normal stress acted normal to the wall. Specifically, the conditions above were replaced by

$$n_i \sigma_{ij} = F_0 \exp\left(\frac{u_k n_k}{L}\right) m_j \tag{2}$$

where F_0 is a magnitude of the fictitious normal stress per unit area at the contact point, L is a characteristic decay length for the force, and m is the unit vector pointing outward from the wall. (If the surface is not in contact, then m is in the same direction as u; if the tissue and the mold have overlapped, m is in the opposite direction to u.) This fictitious normal stress has features that approach the desired condition: as the tissue moves away from the wall, $u_k n_k$ becomes large and negative, and (2) approaches the desired free surface condition. If the tissue moves into the wall, $u_k n_k$ becomes positive, and the normal stress becomes large, pushing the sample away from the wall. No shear stress is generated under any conditions because the stress acts normal to the wall. With $F_0 = 0.007$ Pa and $L = 100$ um, we observed minimal error in all test studies, so those specifications were used.

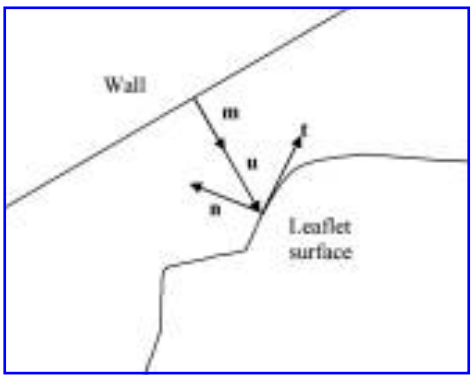

FIG. A1. Reference diagram for penalty scheme.

REFERENCES

1. Mendelson K, Schoen FJ. Heart valve tissue engineering: concepts, approaches, progress, and challenges. Ann Biomed Eng **34,** 1799, 2006.
2. Vesely I. Heart valve tissue engineering. Circ Res **97,** 743, 2005.
3. Barocas V, Girton T, Tranquillo R. Engineered alignment in media-equivalents: Magnetic prealignment and mandrel compaction. J Biomech Eng **120,** 660, 1998.
4. Neidert M, Tranquillo R. Tissue-engineered valves with commissural alignment. Tissue Eng **12,** 891, 2006.
5. Neidert M. Development of a tissue engineered cardiovascular valve. Ph.D. Thesis: Biomedical Engineering. Minneapolis, MN: University of Minnesota, 2003.
6. Vesely I, Boughner D. Analysis of the bending behaviour of porcine xenograft leaflets and of neutral aortic valve material. bending stiffness, neutral axis and shear measurements. J Biomech **22,** 655, 1989.
7. Thubrikar M. The Aortic Valve, 2nd Ed. New York: CRC Press, 1993.
8. Billiar KL, Sacks MS. Biaxial mechanical properties of the native and glutaraldehyde-treated aortic valve cusp: Part II – A structural constitutive model. J Biomech Eng **122,** 327, 2000.
9. Neidert MR, Lee ES, Oegema TR, Tranquillo RT. Enhanced fibrin remodeling *in vitro* with TGF-beta1, insulin and plasmin for improved tissue-equivalents. Biomaterials **23,** 3717, 2002.
10. Grassl ED, Oegema TR, Tranquillo RT. A fibrin-based arterial media equivalent. J Biomed Mater Res **66,** 550, 2003.
11. Long J, Tranquillo R. Elastic fiber production in cardiovascular tissue-equivalents. Matrix Biol **22,** 339, 2003.
12. Barocas V, Tranquillo R. An. anisotropic biphasic theory of tissue-equivalent mechanics: the interplay among cell traction, fibrillar network deformation, fibril alignment, and cell contact guidance. J Biomech Eng **119,** 137, 1997.
13. Ohsumi TK, Flaherty JE, Evans MC, Barocas VH. Three-dimensional simulation of anisotropic cell-driven collagen gel compaction. Biomech Model Mechanobiol 2007 Mar 13; [Epub ahead of print].
14. Tower TT, Neidert MR, Tranquillo RT. Fiber alignment imaging during mechanical testing of soft tissues. Ann Biomed Eng **30,** 1221, 2002.
15. Kiernan J. Histological and Histochemical Methods: Theory and Practice, 3rd Ed. Oxford, UK: Butterworth Heinemann, 1999.
16. Stegemann H, Stalder K. Determination of hydroxyproline. Clinchim Acta **18,** 267, 1967.
17. Starcher BA. Ninhydrin-based assay to quantitate the total protein content of tissue samples. Anal Biochem **292,** 125, 2001.
18. Dombi G, Haut R, Sullivan W. Correlation of high-speed tensile strength with collagen content in control and lathyritic rat skin. J Surg Res **54,** 195, 1993.
19. Kim YJ, Sah RL, Doong JY, Grodzinsky AJ. Fluorometric assay of DNA in cartilage explants using Hoechst 33258. Anal Biochem **174,** 168, 1988.
20. Kim B, Mooney D. Engineering smooth muscle tissue with a predefined structure. J Biomed Mater Res **41,** 322, 1998.
21. Vesely I. Reconstruction of loads in the fibrosa and ventricularis of porcine aortic valves. ASAIO J **42,** M739, 1996.
22. Leyh RG, Schmidtke C, Sievers HH, Yacoub MH. Opening and closing characteristics of the aortic valve after different types of valve-preserving surgery. Circulation **100,** 2153, 1999.
23. Thubrikar MJ, Aouad J, Nolan SP. Comparison of the *in vivo* and *in vitro* mechanical properties of aortic valve leaflets. J Thorac Cardiovasc Surg **92,** 29, 1986.
24. Burriesci G, Howard IC, Patterson EA. Influence of anisotropy on the mechanical behaviour of bioprosthetic heart valves. J Med Eng Technol **23,** 203, 1999.
25. Driessen NJ, Bouten CV, Baaijens FP. Improved prediction of the collagen fiber architecture in the aortic heart valve. J Biomech Eng **127,** 329, 2005.
26. Luo XY, Li WG, Li J. Geometrical stress-reducing factors in the anisotropic porcine heart valves. J Biomech Eng **125,** 735, 2003.
27. Li J, Luo XY, Kuang ZBA. nonlinear anisotropic model for porcine aortic heart valves. J Biomech **34,** 1279, 2001.
28. Holzapfel GA, Gasser TC, Ogden RWA. New constitutive framework for arterial wall mechanics and a comparative study of material models. J Elasticity **61,** 1, 2000.
29. Zulliger MA, Fridez P, Hayashi K, Stergiopulos N. A strain energy function for arteries accounting for wall composition and structure. J Biomech **37,** 989, 2004.
30. van der Kamp A, Nauta J. Fibroblast function and the maintenance of the aortic valve matrix. Cardiovasc Res **13,** 167, 1979.
31. Curran M, Plosker G. Bilayered bioengineered skin substitute (Apligraf): a review of its use in the treatment of venous leg ulcers and diabetic foot ulcers. Biodrugs **16,** 439, 2002.
32. L'Heureux N, Paquet S, Labbe R, Germain L, Auger FAA. completely biological tissue-engineered human blood vessel. [see comment]. FASEB J **12,** 47, 1998.
33. Zund G, Breuer CK, Shinoka T, *et al.* The *in vitro* construction of a tissue engineered bioprosthetic heart valve. Eur J Cardiothorac Surg **11,** 493, 1997.
34. Hoerstrup S, Sodian R, Daebritz S, *et al.* Functional living trileaflet heart valves grown *in vitro*. Circulation **102,** 44, 2000.
35. Shinoka T, Breuer CK, Tanel RE, *et al.* Tissue engineering heart valves: valve leaflet replacement study in a lamb model. Ann Thorac Surg **60,** S513, 1995.
36. Rabkin E, Hoerstrup SP, Aikawa M, Mayer JE Jr. Schoen FJ. Evolution of cell phenotype and extracellular matrix in tissue-engineered heart valves during *in-vitro* maturation and *in-vivo* remodeling. J Heart Valve Dis **11,** 308, 2002; discussion 314.
37. Mol A, Rutten MC, Driessen NJ, *et al.* Autologous human tissue-engineered heart valves: prospects for systemic application. Circulation **114,** I152, 2006.
38. Jockenhoevel S, Chalabi K, Sachweh JS, *et al.* Tissue engineering: complete autologous valve conduit – a new moulding technique. Thorac Cardiovasc Surg **49,** 287, 2001.
39. Williams C, Johnson SL, Robinson PS, Tranquillo RT. Cell sourcing and culture conditions for fibrin-based valve constructs. Tissue Eng **12,** 1489, 2006.
40. Isenberg BC, Williams C, Tranquillo RT. Endothelialization and flow conditioning of fibrin-based media-equivalents. Ann Biomed Eng **34,** 971, 2006.
41. Cataloglu A, Clark RE, Gould PL. Stress analysis of aortic valve leaflets with smoothed geometrical data. J Biomech **10,** 153, 1977.

42. Thubrikar M, Piepgrass WC, Deck JD, Nolan SP. Stresses of natural versus prosthetic aortic valve leaflets *in vivo*. Ann Thorac Surg **30,** 230, 1980.
43. Lee TC, Midura RJ, Hascall VC, Vesely I. The effect of elastin damage on the mechanics of the aortic valve. J Biomech **34,** 203, 2001.
44. Liu W, Jawerth L, Sparks E, *et al.* Fibrin fibers have extraordinary extensibility and elasticity. Science **313,** 634, 2006.
45. Gildner C, Lerner A, Hocking D. Fibronectin matrix polymerization increases tensile strength of model tissue. Am J Physiol Heart Circ Physiol **287,** H46, 2004.
46. Sutherland FW, Perry TE, Yu Y, Sherwood MC, *et al.* From stem cells to viable autologous semilunar heart valve. Circulation **111,** 2783, 2005.
47. Schmidt D, Mol A, Breymann C, *et al.* Living autologous heart valves engineered from human prenatally harvested progenitors. Circulation **114,** I125, 2006.

Address reprint requests to:
Robert T. Tranquillo, Ph.D.
Department of Biomedical Engineering
7–114 BSBE
312 Church St SE
University of Minnesota
Minneapolis, MN 55455

E-mail: tranquillo@cems.umn.edu